

Результаты исследований, выполненных Лабораторией в рамках проекта ТРАКТ 2018

(<http://ru.niersc.spb.ru/trakt-2018.html>)

1. Factors, determining “Heat Island” in city of Apatity during winter. Relation of land surface temperature (LST) and air temperature at the 2 m level above surface

Authors: S.G.Kritsuk, V.I.Gornyy, T.A.Davidan

The simplified geographical scheme of the region of investigation was used for geolocation of satellite data (fig. 1).

14 scenes of LandSat satellite were selected (Table 1) and processed. LST was retrieved. The example is exhibited at fig. 2.

Table 1 – Satellite data used in the step 3

No	Satellite	Date	Max air temp.*, °C	No	Satellite	Date	Max air temp.*, °C.
1	LandSat 8	22.10.2014	-4.7	8	LandSat 8	13.03.2017	2.3
2	LandSat 8	07.11.2014	-5.4	9	LandSat 8	20.03.2017	-2.0
3	LandSat 8	04.02.2015	-16.3	10	LandSat 8	19.02.2018	-8.1
4	LandSat 8	22.03.2015	-5.2	11	LandSat 8	07.03.2018	-11.0
5	LandSat 8	01.03.2016	-7.3	12	LandSat 8	12.02.2018	-8.2
6	LandSat 8	31.01.2017	-10.1	13	LandSat 7	08.03.2018	-12.3
7	LandSat 8	13.03.2017	2.3	14	LandSat 8	14.03.2018	-5.7

*Daily maxima air temperatures were obtained from meteorological station “Apatity” WMO 22213

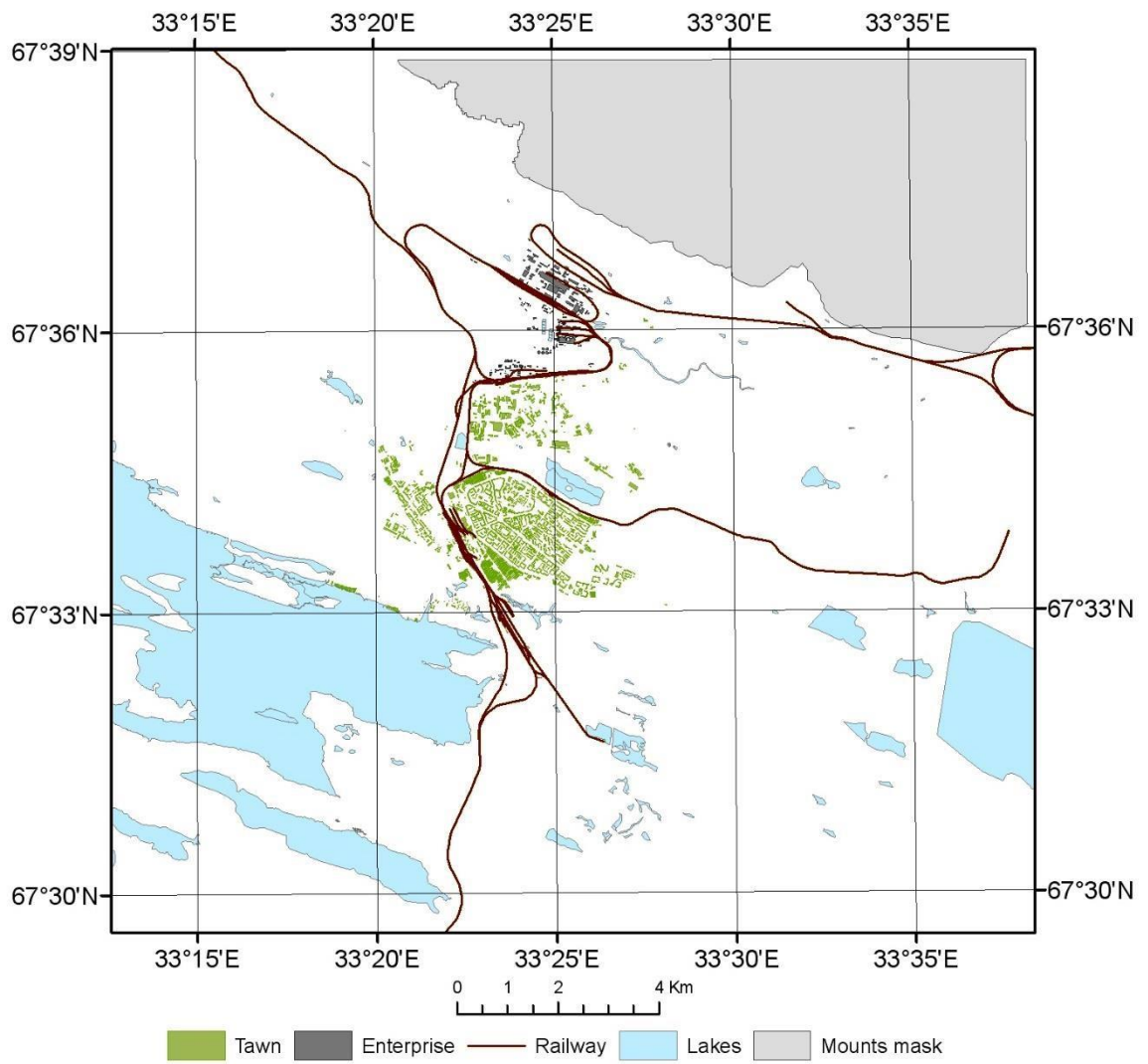


Figure 1. Geographical scheme of the region of investigation.

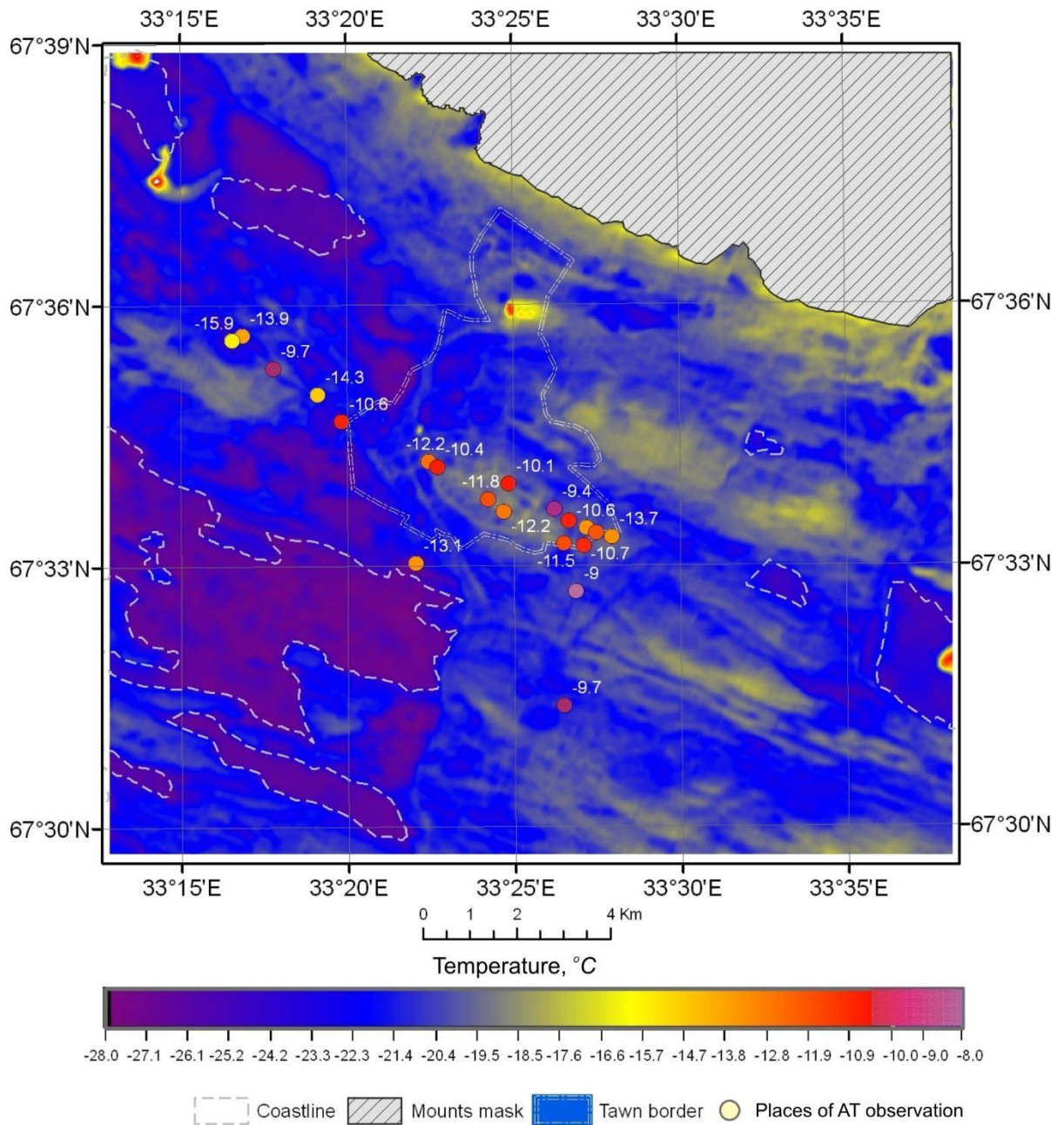


Figure 2. Map of LST, retrieved from Landsat 8 data. 12:00 Moscow time, 07.03.2018.

Additionally, the ASTER digital elevation model (DEM) (fig. 3 B), the results of air temperature measurements by automatic meteorological station and 24 air temperature loggers: air temperature time series, recorded by the experimental monitoring network of Urban Heat Island Arctic Research Campaign (Konstantinov, Varentsov and Esau, 2018) were used for the additional analysis.

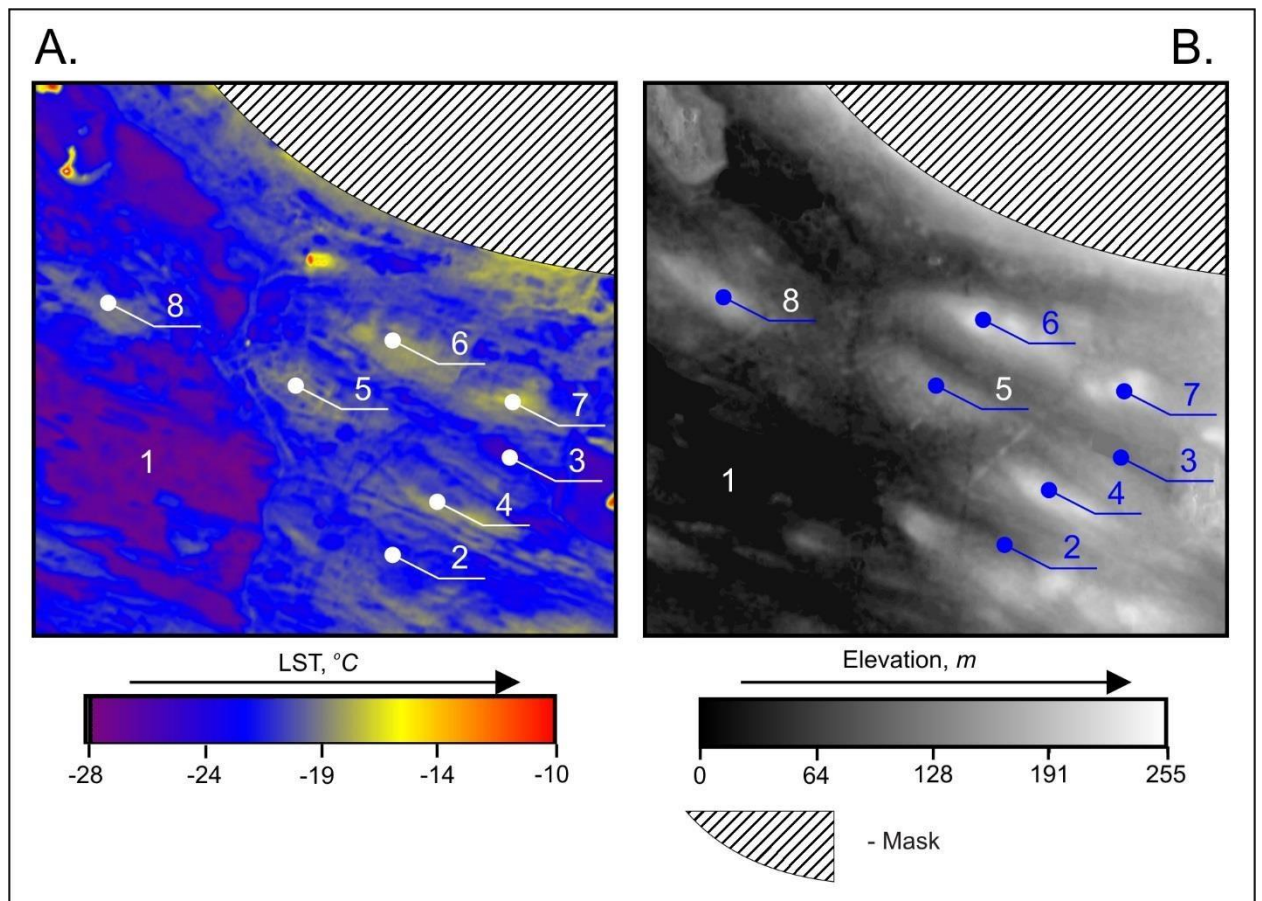


Figure 3. A) Map of LST, retrieved from LandSat 8 data. 12:00 Moscow time, 07.03.2018. B) Digital elevation model (ASTER).

First of all, the correlation between LST (LandSat data) and land surface elevation (ASTER DEM) was analyzed (fig. 2-4).

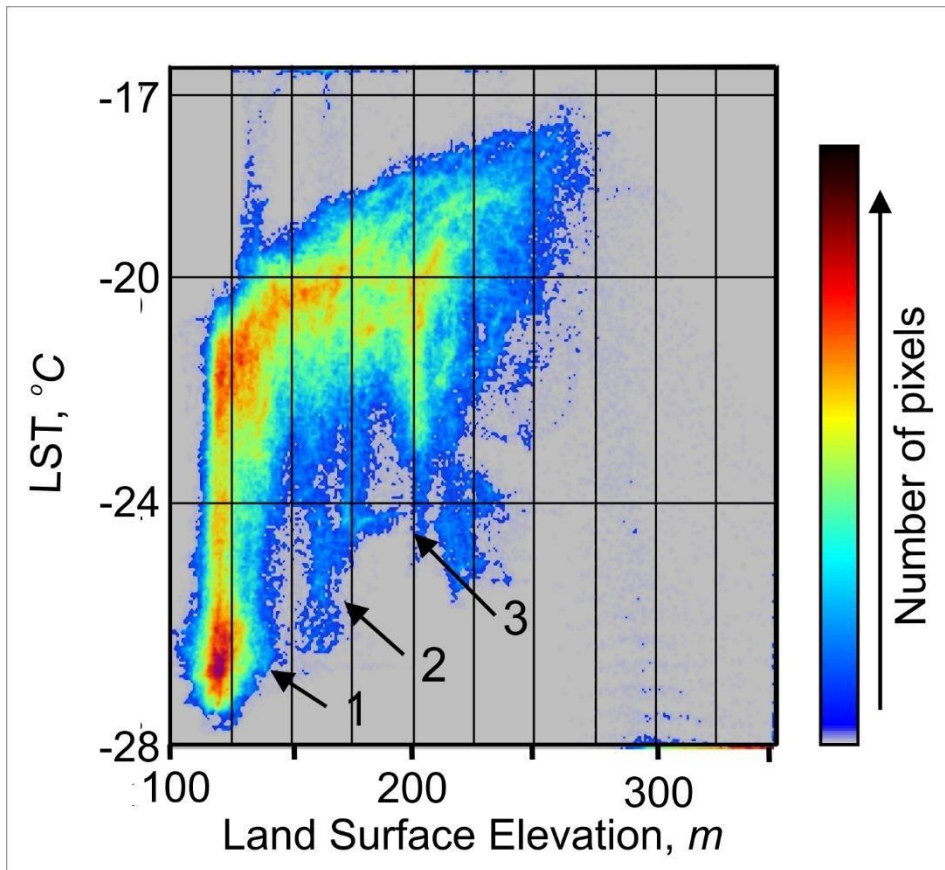


Figure 4. Scatter plot of LST and Land Surface Elevation (Date: March 07, 2018. Time: 12:00 Moscow time. Lowlands: land surface elevations no more than 350 m).

One can notice at the fig. 4 the unusual vertical “icicles” (1, 2, 3 at the fig. 4), which indicate areas where LST suddenly deviates from the general tendency and reaches minima in some places with lower elevation levels: 118 - 140 *m* (1 at fig. 3, 4); 160 - 180 *m* (2 at fig. 3, fig. 4); 200 - 225 *m* (3 at fig. 3 fig. 4). This regularity clear seen at the histogram of elevations of surface relief (fig. 4), too.

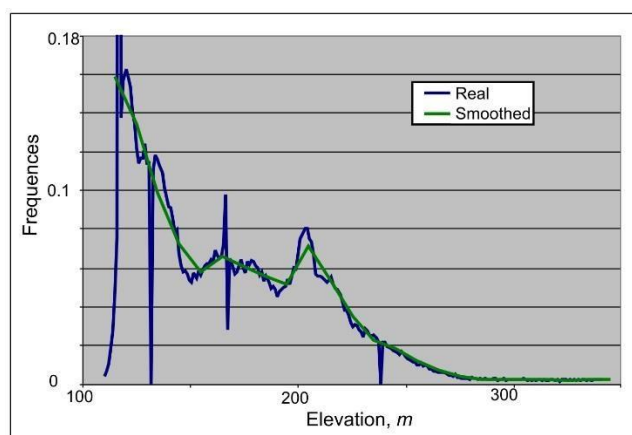


Figure 4. Histogram of relief elevation.

Elevations about 120 *m* are located near by the Imandra Lake, ice LST of which reach. Other two local maxima correspond to two tailing ponds of the obage fabric.

Elevations about 120 *m* are located near by the Imandra Lake are characterised by very low LST. On the ice of Imandra Lake LST reach -27°C . Other two local maxima correspond to two tailing ponds.

This strange shape of scatter cloud points out to the different mechanisms of LST formation in areas with the general tendency and in places which created "icicles". The brief analysis of the fig. 3 leads to the idea that territories, formed the "icicles" are valleys in the relief of the surface. These valleys are stretching in the NE direction to Imandra Lake (see 2, 3 at fig. 3 B). This regularity confirms the hypothesis about cold air flows from the highlands (4, 5, 6, 7, 8 at fig. 3 B) to the negative forms of surface relief (1, 2, 3 at fig. 3B) in the winter in conditions of low wind speed and radiative cooling (Konstantinov et al., 2015; Demin et al., 2016). The map of LST (fig. 2) shows the big areas of very low LST of ice cover of Imandra Lake (1 at fig. 3). This effect was partially investigated in (Bin Cheng et al., 2014). The main conclusion was that the problem is quite complex for modelling, because of big number of factors, influencing the process. We consider that the radiative cooling is the main mechanism, forming very low ice surface temperature. Thus, the regular satellite observations combined with modelling could be useful for this problem solution. In the same time highlands indicated by the positive LST anomalies (4, 5, 6, 7, 8 at fig. 3 B). It is necessary to note that amplitude of LST anomaly above the city of Apatity reaches $+1.5^{\circ}\text{C}$. But the highest LST inside the city of Apatity reaches -19.0°C indicates the major streets and apartment buildings. It can be due to few reasons: - vertical walls solar heating; - snow cleaning on major roads; - underground heating pipelines of house heating system Conclusions:

- Most probably, there are two mechanisms of LST formation at the investigated territory. The first one forms LST at highlands by radiative and convective heat

exchange between land surface and atmosphere. The second one forms low LST in depressions of surface relief due to the wind from slopes. This air motion delivers cold air to the depressions. After that radiative cooling in conditions of atmosphere inversion makes LST extremely low. That is why the statistical relations between LST and air temperature at the height 2 m have to be different for highlands and lowlands;

- The above conclusion must be taken into account in the process of LST modelling.

2. Relation of LST and air temperature at the 2 m level above surface (AT)

Authors: S.G.Kritsuk, V.I.Gornyy.

The conclusion that there is no confidence correlation between AT recorded by loggers in the city of Apatity (fig. 6) with land surface elevation was done after brief analysis. After that the correlation between AT (loggers) and LST (LandSat) was investigated (fig. 6). Suddenly the strong correlation was discovered for March 7, 2018 (fig. 7) and nonconfidential links between AT and LST was obtained for March 8, 2018. Analysis of meteorological data showed the stable atmospheric conditions during March 7 without wind, but on March 8 the temperature became higher, as well as the speed of wind.

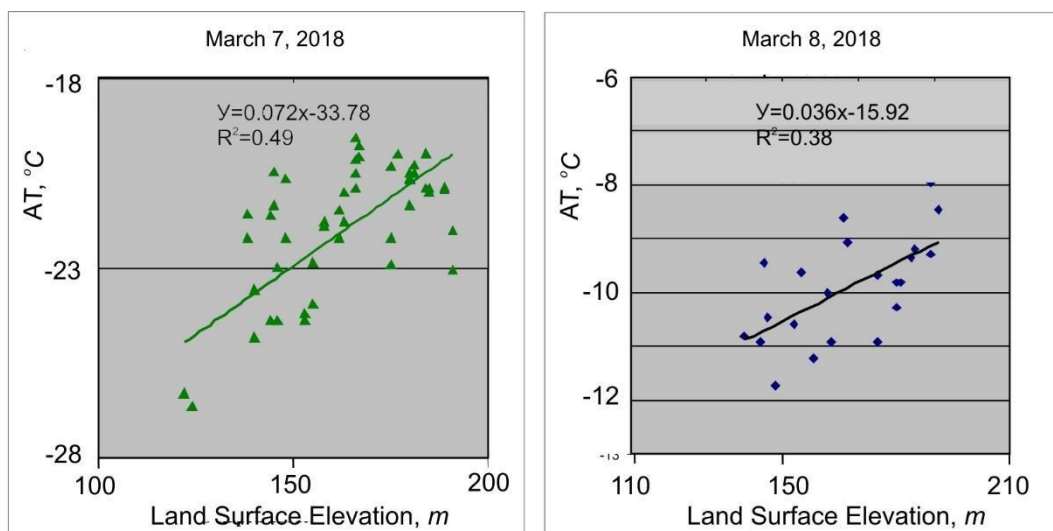


Figure 6. Correlation AT (loggers in Apatity) and land surface elevation.

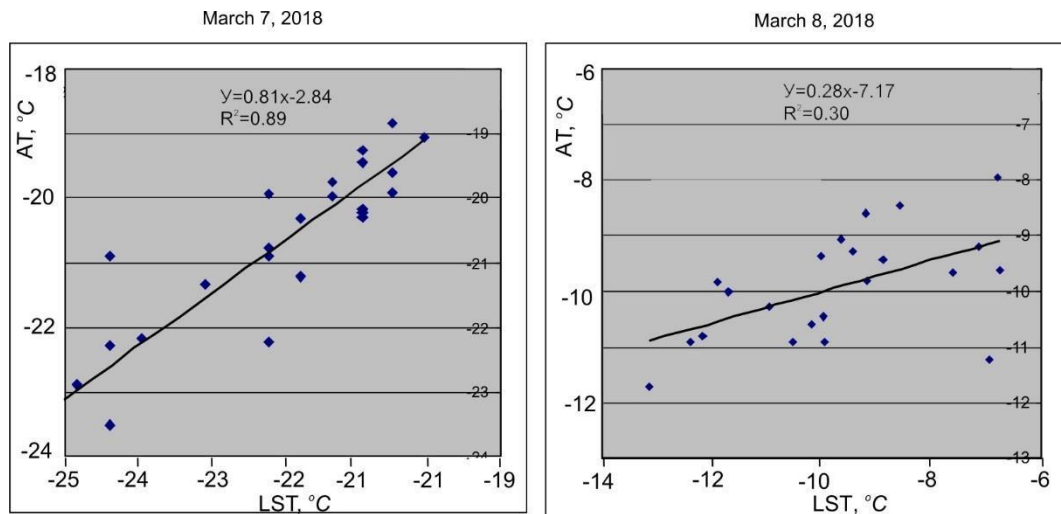


Figure 7. Correlation AT (loggers in Apatity) and LST (LandSat).

The additional analysis showed that during the polar winter the best correlation between AT and LST observed in conditions of small wind speed and radiative cooling (fig. 7).

Conclusion:

- The method of high-resolution mapping of AT by using infrared thermal satellite survey in cold season of polar regions must produce precise result only in conditions of small wind speed and radiative cooling.

3. Satellite method of AT mapping with high spatial resolution *Authors:*

S.G.Kritsuk, V.I.Gornyy.

A high spatial resolution satellite imagery depending of number of satellites and system of satellite targeting has repetition from 1~ 15 days. But the satellite survey of polar regions is very difficult, because of hard cloudiness. That is why, it is very difficult to get high quality image in polar region during winter. The main

idea of our method of AT mapping in high spatial resolution mode is based on the technique of data fusion, which were recorded by satellites (spatial information) and by standard meteorological stations (time series). Thus, the correlation for each pixel of LST maps (LandSat results, the table 1) and AT (daily maxima AT, the table 1) was done (fig. 8).

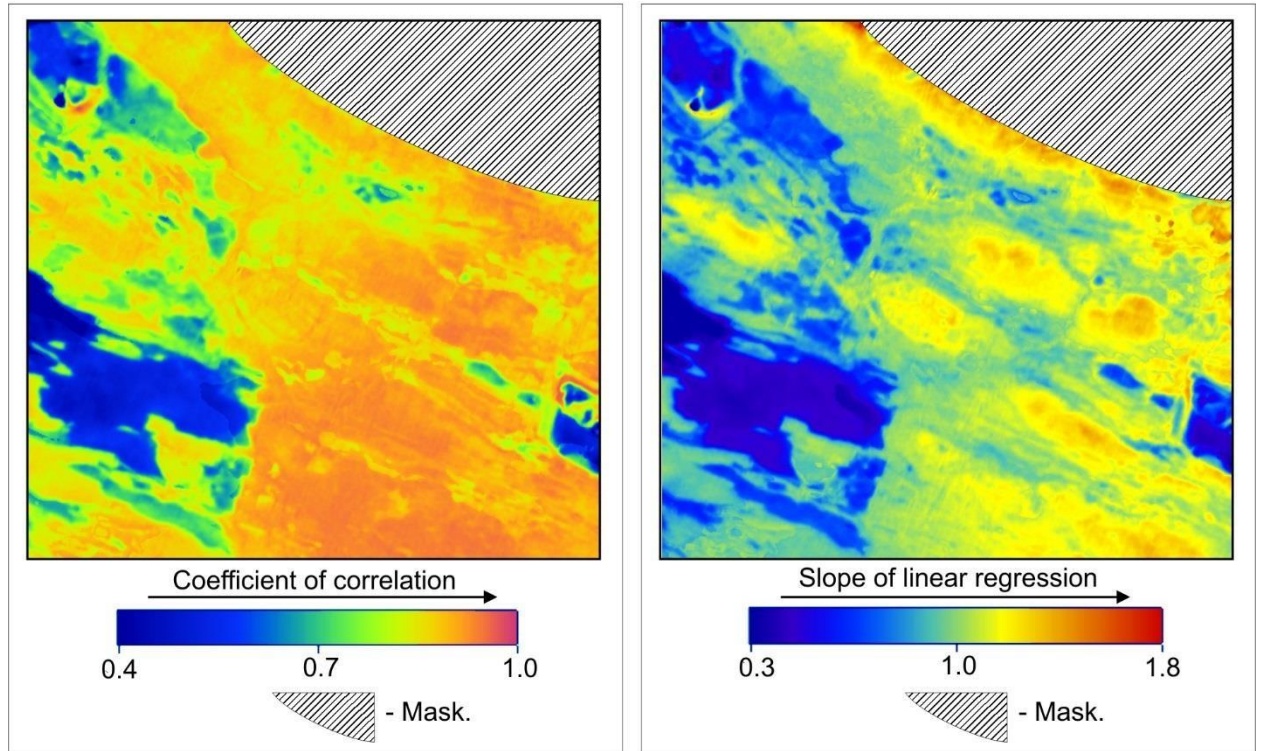


Figure 8. A) Map of coefficients of correlation between LST (LandSat) and maximal AT (Meteostation). B) Map of slopes of linear regression between LST (LandSat) and maximal AT (Meteostation).

Analysis of results of correlation (fig. 8) showed that the confidence of the slope of linear regression between LST and daily maxima of AT is enough for the practical mapping of AT with the spatial resolution of LandSat images (~100 m). Additional analysis showed that the high level of AT mapping reliability can be reached in conditions of stable stratification of lower atmosphere (fig. 9). The best results of AT mapping were obtained for 01-st of February and 5-th of February, when R^2 were not lower than 0.82 (fig. 9 and fig. 10). But on 6-th of February stability of lower atmosphere became destroying, but the contrast of AT stilled significant, but, R^2 became lower than 0.5 (see fig. 8).

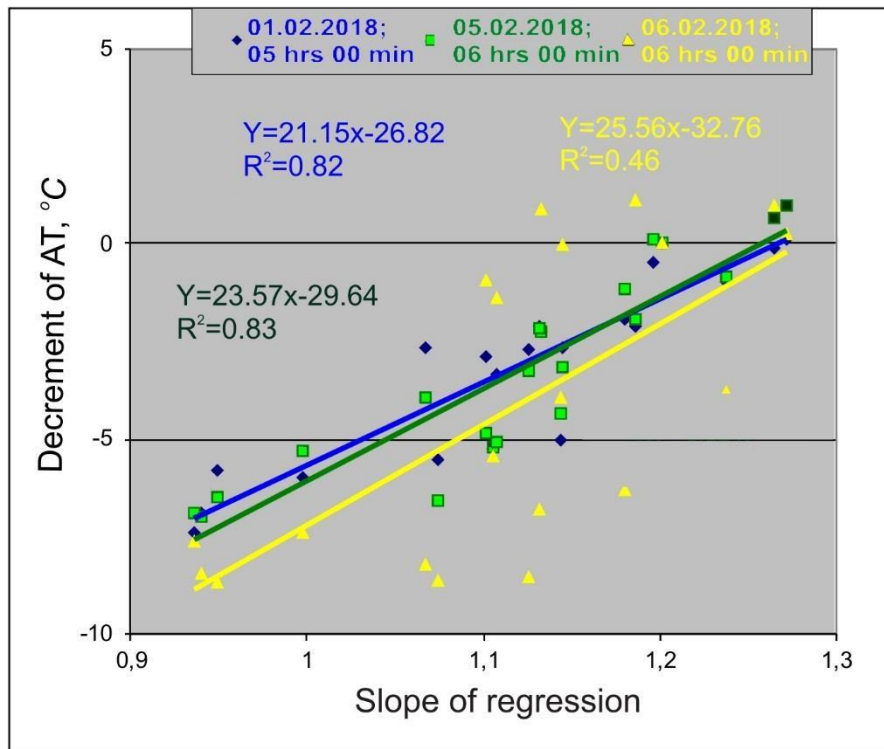


Figure 8. Regressions used for AT mapping. Decrement AT = AT-AT_{AWS}. AWS - automatic weather station.

Finally, we compiled maps of AT with the spatial resolution $\sim 100\text{ m}$ for 1-st, 3-d, and 5-th of February 2018 (see the example at fig. 11).

The most reliable AT's lay inside the diapason between -27°C – -17°C . The root square error (RSE) was estimated as $\text{RSE}=1^{\circ}\text{C}$ by comparison the results of AT mapping with really observed AT by loggers. The estimated precision of AT high spatial resolution mapping is enough well, especially considering that the temperature sensitivity of loggers was 0.5°C and the real temperature sensitivity of LandSat infrared thermal channel for the low LST is no better that 0.5°C .

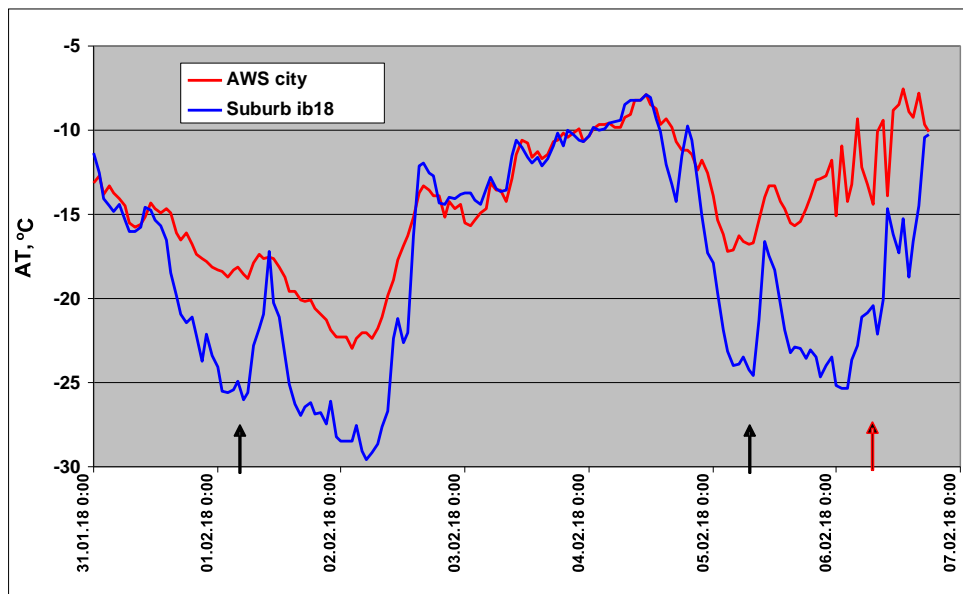


Figure 10. Variations of the surface air temperature at the urban AWS site (red line) and at the nearest suburb of the city of Apatity (blue line). Black arrows appointing dates with the high confidence of AT mapping, red arrow – the low confidence level of AT mapping.

Visual analysis of AT map (fig. 11) showed that the AT of the city of Apatity is not higher than other tops of hills. Detailed investigation of the Apatity anomaly internal structure proved the above-mentioned conclusion that streets and apartment buildings indicates by the highest temperatures at the background of football fields, green zones and nearest suburbs. But this AT anomaly lays in the limits of similar AT anomalies indicating other tops of hills.

Conclusions:

- The developed method of AT mapping is correct for polar region winter in stable atmosphere conditions with strong radiative cooling.
- The SRE of suggested and verified by the ground truth method of AT mapping with high-resolution by using satellite infrared thermal imagery and standard meteorological observations is enough to needs of high-resolution environmental impact assessment and management.

- The one of advantages of the developed and applied method is the possibility to map AT for dates, when satellite survey was not done, because of low satellite repetition.

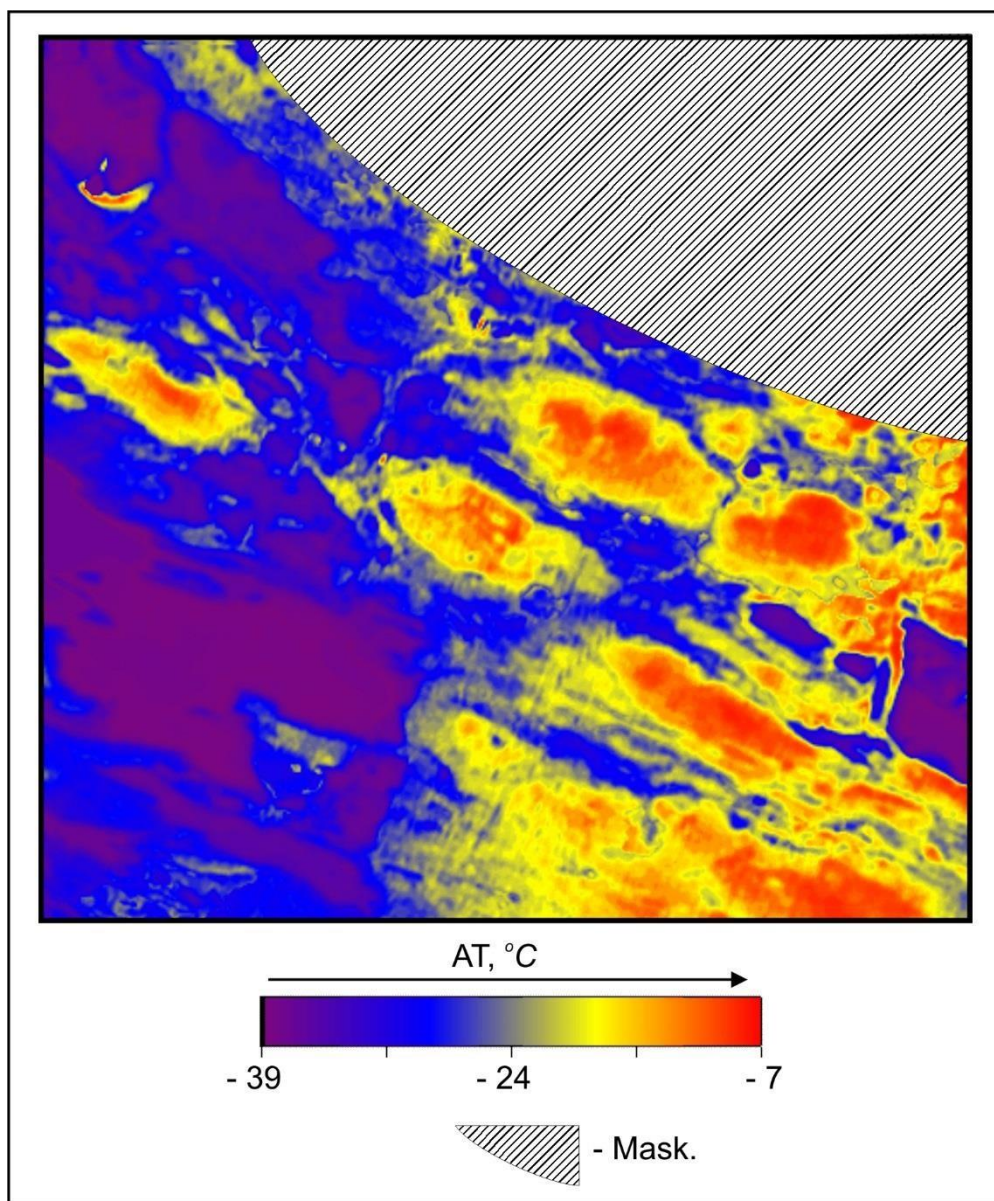


Figure 11. The map of AT compiled on 1-st of February 05 hrs 00 min of Moscow time. Spatial resolution ~ 100 m). (on the base of Landsat and meteorological data).

5. Air-technogenic pollution of snow cover by the dust of obage fabric *Authors:*
S.G.Kritsuk, V.I.Gornyy, T.A.Davidan

The problem of air-technogenic pollution by a dust from obage fabric is quite actual. It was investigated by the in-situ observations and by mathematical simulations of the dust transfer by winds (Baklanov, Rigina, 1998; Masloboev et al., 2016). We used LandSat 8 satellite data to map air-technogenic pollution of snow. The normalized-differece snow index (NDSI) was used for that. The NDSI is defined as the difference of reflectances observed in a visible band such as MODIS band 4 (0.555 μm) and a short-wave infrared band such as MODIS band 6 (1.640 μm) divided by the sum of the two reflectances (Salomonson, Appel, 2004):

$$NDSI = \frac{R_{0.66} - R_{1.6}}{R_{0.66} + R_{1.6}} \quad (2)$$

Effectiveness of NDSI application for air-technogenic pollution mapping was verified on a snow cover of Onega Lake near city of Petrozavodsk (Krutskih, Kravchenko, 2018) in the natural conditions similar to Imandra Lake. The map of NDSI was compiled by processing the LandSat 8 (March 11, 2016) scene (fig. 13). As a result, the significant air-technogenic pollution by the dust, caused by explosions in mining open custs (2 at fig. 13) was discovered on the ice-snow cover of Umbosero lake. The similar pollution was noticed on the Imandra Lake ice cover (4 at fig. 13) and near tailing ponds of the Apatity Obage Fabric. Additionally, we compiled the map of normalize difference vegetation index (NDVI) (fig. 14), because the dust, containing a big amount of phosphorus in apatite, can initiate eutrophication of water in the Imandra Lake.

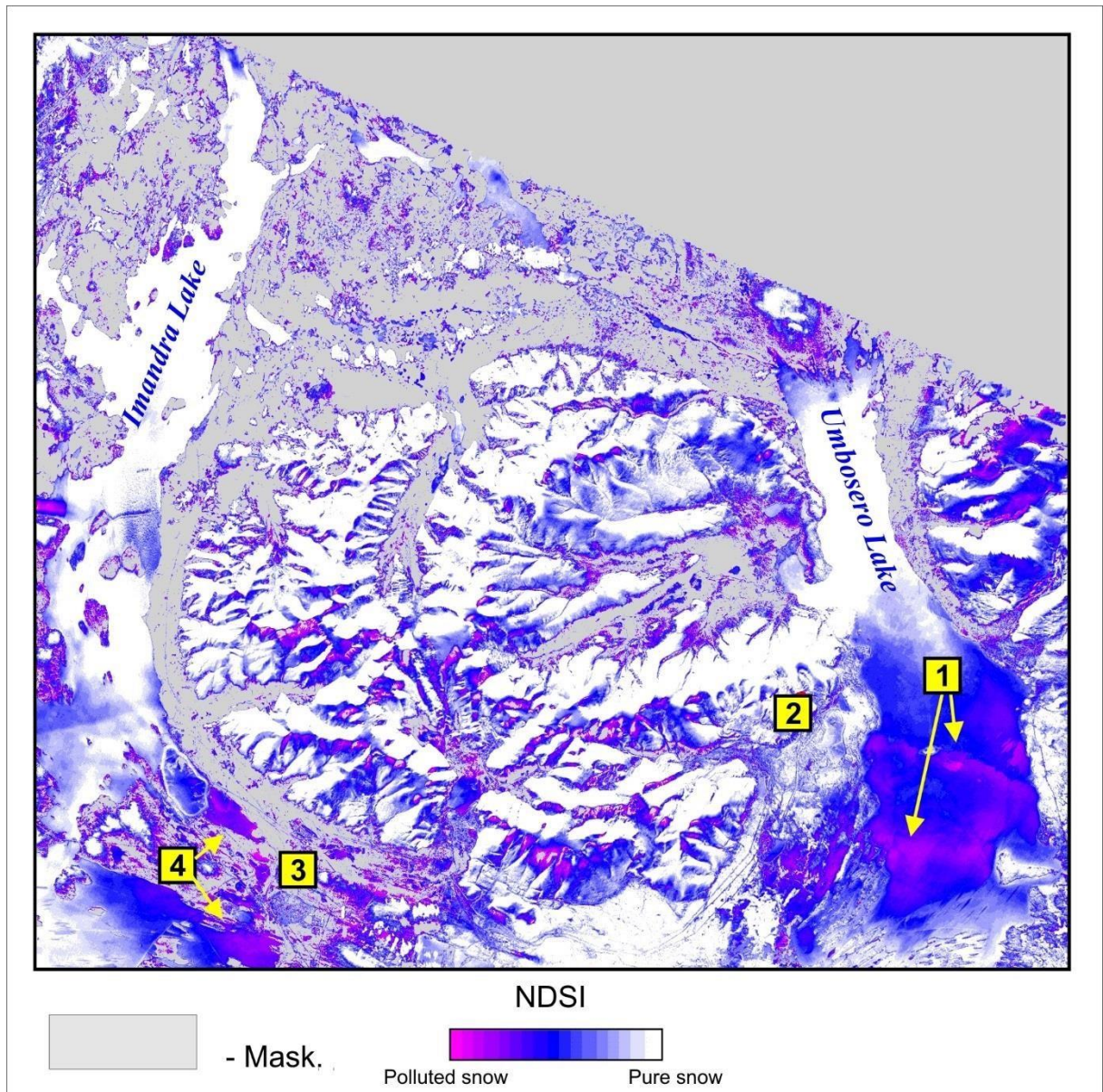


Figure 13. Map of NDSI. Low quantities of NDSI indicate snow pollution. 1 - Air-technogenic pollution by dust emitted by explosions in the queries. 2 - Queries. 3 - The city of Apatity. 4 - Airtechnogenic pollution by dust emitted by obage fabric.

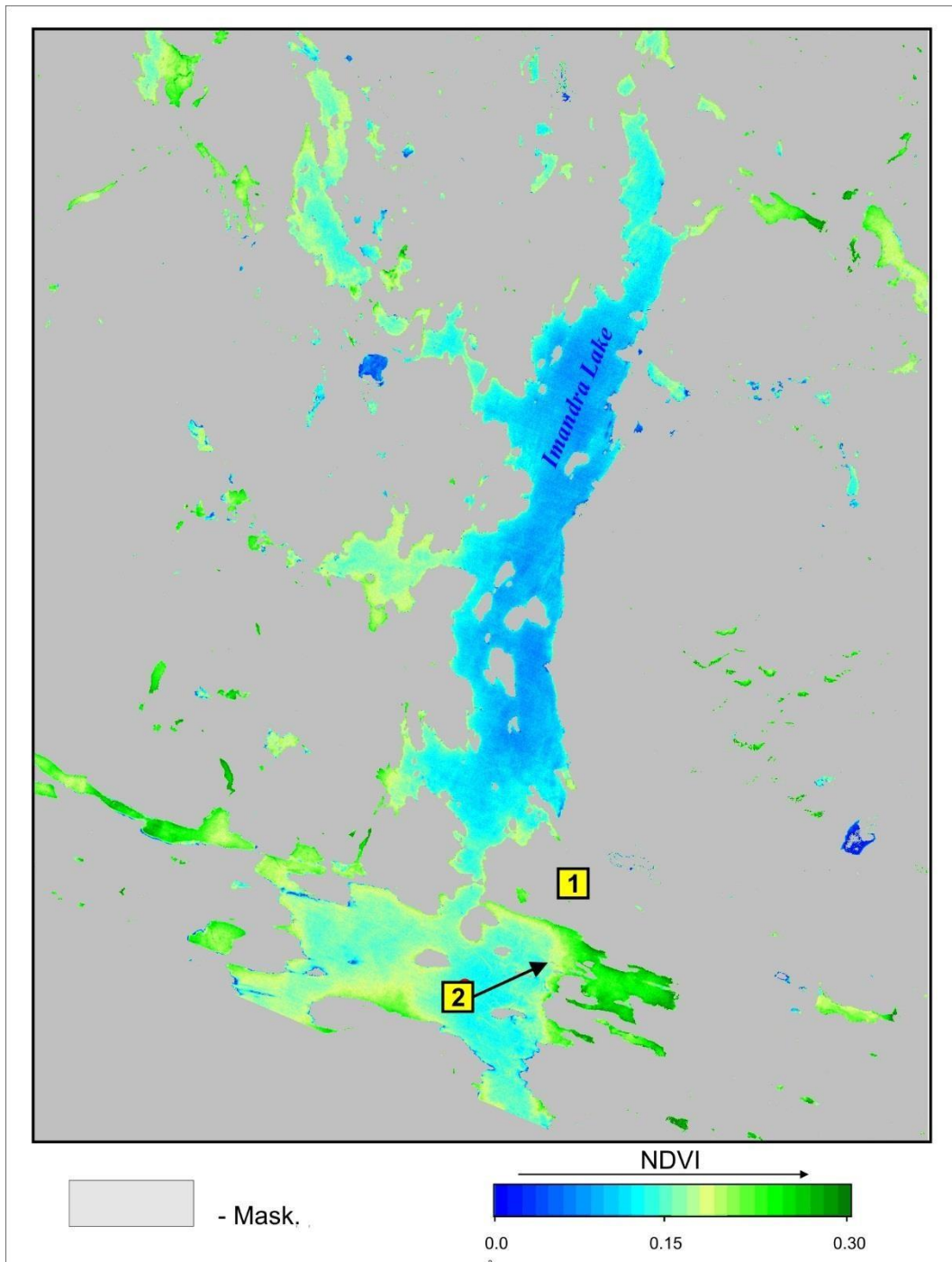


Figure 14. Map of NDVI. Landsat 8, August 10, 2017. 1 – the city of Apatity. 2. High NDVI in waters of Imandra Lake near the city of Apatity.

The map of NDVI (fig. 14) showed that the nearest to the city of Apatity gulf of the Imandra Lake indicates by high NDVI (2 at fig. 14). The analysis of detailed maps (fig. 15) showed that the areas of the intensive dust pollution and high NDVI

are coincided. It proved suggestion that dust transportation by wind can initiate eutrophication of Imandra Lake water.

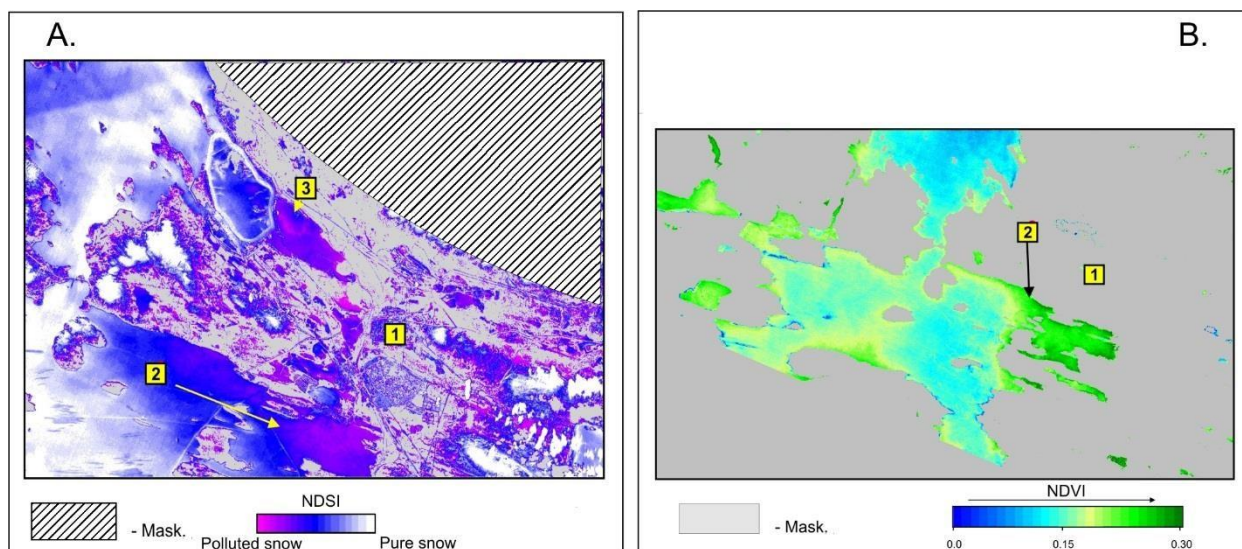


Figure 15. A) Map of NDSI. B) Map of NDVI. 1 - the city of Apatity. 2 - polluted gulf of Imandra Lake. 3 - dust pollution from tailing pond.

Conclusions:

- NDSI and NDVI maps are effective for monitoring of dust pollution in the region of the city of Apatity;
- It seems promising to combine NDSI and NDVI mapping with mathematical simulation of the dust wind transfer.

References

1. BAKLANOV A. and RIGINA O. Environmental modelling of dusting from the mining and concentration sites in the Kola Peninsula, Northwest Russia // The XI World Clear Air and Environment Congress, 14-18 Sept. 1998, Durban, South Africa, IUAPPA-NACA, Vol. 1, 4F-3. Pp. 1-18.
2. Bin Cheng, Timo Vihma, Laura Rontu, Anna Kontu, Homa Kheyrollah Pour,
3. Claude Duguay & Jouni Pulliainen. Evolution of snow and ice temperature, thickness and energy balance in Lake Orajärvi, northern Finland // *Tellus A* 2014, 66, 21564, <http://dx.doi.org/10.3402/tellusa.v66.21564>
4. Gornyy V. I., Kricuk S. G., Latypov I. SH., Tronin A. A., SHilin B. V. Distancionnyj izmeritel'nyj monitoring teplopoter' gorodskih i promyshlennyh aglomeracij (na primere Sankt Peterburga i Hel'sinki) (Remote measurement monitoring of urban heat losses (on

- example of Saint-Petersburg and Helsinki) // *Teploeffektivnye tekhnologii*. No 2. 1997. pp. 17–23.
5. Gornyy V. I., Kritsuk S. G., Latipov I.Sh., Tronin A. A., Shilin B. V. Estimation of Nuclear Power Plants Influence on the Baltic Sea Thermal State by Using Infrared Thermal Satellite Data // *Intern. J. Remote Sensing*. 2000. V. 21. Iss. 12. P. 2479–2496.
 6. Gornyy V.I., Kritsuk S.G., Latypov I.Sh., Tronin A.A., et al. Thermophysical properties of land surface in urban area (by satellite remote sensing of Saint-Petersburg and Kiev) // *Sovremennyye problemy distantsionnogo zondirovaniya Zemli iz kosmosa*. 2017. Vol. 14. No 3. pp. 51–66.
 7. Demin V.I., Kozelov B.V., Elizarova N.I., Men'shov YU.V., Konstantinov P.I. ROL' REL'EFA V VOZNIKNOVENII «OSTROVA TEPLA» V GORODE APATITY (The role of a surface relief for the “Heat Island” formation in the city of Apatity) // *Fundamental'naya i prikladnaya klimatologiya* 2016. №2. Ss. 95-106. (In Russian).
 8. Demin, B. V. Kozelov, N. I. Elizarova, YU. V. Men'shov V. I. Vliyanie mikroklimata na tochnost' ocenki gorodskogo "ostrova tepla" (Influence of microclimate on the precision of city “heat island” estimation) / // *Trudy Glavnoj geofizicheskoy observatorii im. A.I.Voejkova*. — 2017. — No 584. — pp. 74–93.
 9. Konstantinov P. I., Grishchenko M. Y., and Varentsov M. I. Mapping Urban Heat Islands of Arctic Cities Using Combined Data on Field Measurements and Satellite Images Based on the Example of the City of Apatity (Murmansk Oblast) // *Izvestiya, Atmospheric and Oceanic Physics*, 2015, Vol. 51, No. 9, pp. 992–998.
 10. Konstantinov P., Varentsov M. and Esau I. A high-density urban temperature network deployed in several cities of Eurasian Arctic. *Environ. Res. Lett.* 13 (2018) 075007.
 11. Krutskih N.V., Kravchenko I.YU.. Ispol'zovanie kosmosnimkov Landsat dlya geoekologicheskogo monitoringa urbanizirovannyh territorij (The use of Landsat satellite images for geocological monitoring of urbanized areas) // *Sovremennyye problemy distantsionnogo zondirovaniya Zemli iz kosmosa*. 2018. Vol. 15. No 2. pp. 159-168
 12. Masloboev V. A., Baklanov A. A., Amosov P. V.. REZUL'TATY MODELIROVANIYA PROCESSOV PYLENIYA HVOSTOHRANILISHCH (Results of modelling of dusting process above tailing ponds) // *VESTNIK Kol'skogo nauchnogo centra RAN* 1/2016(24). pp. 59-68.
 13. V.V. Salomonson, I. Appel. Estimating fractional snow cover from MODIS using the normalized difference snow index // *Remote Sensing of Environment* 89 (2004). pp. 351–360
 14. Sekioka M., Yuhara K. Heat Flux Estimation in Geothermal Areas Based on the Heat Balance of Ground Surface // *J. Geophysical Research*. 1974. V. 79. No. 14. P. 2053–2058.